

Structural investigation of the VEGF receptor interaction with a helical antagonist peptide[†]

Donatella Diana,^a Rossella Di Stasi,^a Lucia De Rosa,^a Carla Isernia,^b Luca D. D'Andrea^a and Roberto Fattorusso^{b*}

Angiogenesis is mainly regulated by the vascular endothelial growth factor (VEGF), a mitogen specific for endothelial cells, which binds two tyrosine kinase receptors, VEGFR1 and VEGFR2, on the surface of endothelial cells. Molecules targeting VEGF receptors are attractive to pharmacologically treat diseases associated with angiogenesis or to be used as probes in angiogenesis imaging. Recently, we reported a designed peptide targeting VEGF receptors and able to inhibit the VEGF-angiogenic response *in vitro* and *in vivo*. In this study, we employed NMR and molecular modeling methodology to investigate the molecular determinants of the interaction peptide-receptor. In particular, the peptide binding site on VEGFR1 domain 2 and the residues involved in receptor recognition have been determined. These results provide significant information to develop a new class of molecules able to recognize the VEGF receptors overexpressed in pathological angiogenesis. Copyright © 2013 European Peptide Society and John Wiley & Sons, Ltd.

Keywords: VEGF; angiogenesis; NMR; peptide; interactions

Introduction

The vascular endothelial growth factor (VEGF) is a homodimeric cytokine-regulating angiogenesis mainly acting on endothelial cells (EC) [1]. VEGF interacts with two tyrosine kinase transmembrane receptors (VEGFR1/Flt-1 and VEGFR2/KDR) on the surface of EC. VEGF receptors contain an extracellular region, composed of seven Ig-like domains, a short transmembrane helix, and the intracellular kinase domain. The high-affinity binding of VEGF to the extracellular region induces receptor dimerization and activation-stimulating transphosphorylation of the intracellular kinase domain. The phosphorylated tyrosines act as docking sites for the recruitment of intracellular proteins, which in turn activate signaling pathways, involving key mediators, such as Akt and ERK1/2, ending up in EC proliferation, migration, and survival [2]. Structural and biochemical studies showed that VEGF binding to VEGFR1 mainly involved domain 2 (VEGR1_{D2}) [3], whereas binding to VEGFR2 required receptor domains 2 and 3[4,5].

Many studies have been devoted to find novel molecules able to modulate VEGF signaling targeting VEGF-VEGF receptor interaction [6–8]. Such molecules have potential applications in the treatment of cancer and other pathologies depending on excessive angiogenesis [9–11] to stimulate angiogenesis [11,12] and for the imaging of VEGF receptors [13,14].

Over the last several years, we reported the structural and biological properties of several VEGFR binder peptides designed on VEGF regions involved in VEGFR recognition such as the N-terminal helix (residues 17–25) [15–23] and the β -hairpin encompassing residues 79–92 [24].

Particularly, we have described the design, structure, and functional characterization of a novel VEGF antagonist helical peptide [21]. We showed that this peptide, MA, assumes in water a well-defined helical conformation, binds to VEGF receptors, and inhibits the VEGF biological activity on ECs. Furthermore, *in vivo* experiments showed that MA inhibits VEGF-induced capillary

formation and tumor growth. Thus, MA represents a candidate for the treatment of diseases associated with excessive VEGF-dependent angiogenesis.

To identify the molecular details of the interaction between VEGF receptor and MA, we report the structural characterization of the interaction between MA and VEGFR1_{D2} by using NMR spectroscopy and molecular modeling studies. In particular, MA selectivity and binding to the VEGFR1_{D2} has been evaluated by means of NMR chemical shift perturbation experiments, which allow for the identification of the amino acid residues of VEGFR1_{D2} involved in MA recognition. Furthermore, the interaction between MA and VEGFR1_{D2} was monitored by one-dimensional NMR saturation transfer difference (STD) to define the binding epitope of the ligand. Finally, a structural model of VEGFR1_{D2}-MA complex has been derived by molecular modeling on the basis of NMR-derived constraints.

Materials and Methods

Chemicals

Fmoc-protected amino acids and coupling reagents were purchased from Inbios (Naples, Italy). Rink amide MBHA resin was obtained from Merck (Nottingham, UK). Peptide synthesis

* Correspondence to: Roberto Fattorusso, Dipartimento di Scienze Ambientali, Seconda Università di Napoli, Via Vivaldi 43, Caserta, Italy. E-mail: roberto.fattorusso@unina2.it

[†] Special issue devoted to contributions presented at the 13th Naples Workshop on Bioactive Peptides, June 7–10, 2012, Naples.

^a Istituto di Biostrutture e Bioimmagini, CNR, Via Mezzocannone 16, Napoli, Italy

^b Dipartimento di Scienze Ambientali, Seconda Università di Napoli, Via Vivaldi 43, Caserta, Italy

solvents *N,N*-DMF and DCM were obtained, respectively, from Romil (Cambridge, UK) and Sigma-Aldrich (Milan, Italy) with the lowest water content and used without further purification. Piperidine was from Biosolve (Valkenswaard, Netherlands), and *N,N*-DIPEA from Romil (Cambridge, UK), and acetic anhydride triisopropylsilane, ethanedithiol, acetonitrile (CH₃CN), and TFA were from Sigma-Aldrich.

SPPS

MA peptide (acetyl-KLTWMEYLQLAYKGI-amide) was synthesized on Rink amide MBHA resin (0.5 mmol/g) using standard Fmoc/tBu chemistry. Fmoc deprotection was performed by washing the resin two times for 5 min with a solution of 30% piperidine in DMF, and coupling reactions were performed with 10 equiv of Fmoc-amino acid and 9.9 equiv of HBTU/HOBt, 20 equiv DIPEA in DMF for 45 min at room temperature; capping step (1 × 5 min) was performed with a solution of acetic anhydride (0.5 M)/HOBt (0.015 M)/DIPEA (0.125 M) in DMF. Each step was followed by five washing with DMF for 1 min. Peptide cleavage was performed using a mixture of TFA/H₂O/ethanedithiol/triisopropylsilane (94:2.5:2.5:1 v/v/v/v) for 3 h at room temperature. Resin was separated by filtration, and the filtrate was precipitated with cold diethyl. The precipitate was separated by centrifugation, solubilized in water, and lyophilized.

Peptide Purification and Analysis

Peptide purifications were carried out by RP-HPLC on the Shimadzu (Kyoto, Japan) LC-8A system, equipped with a UV-vis detector SPD-10A using a semi-preparative Phenomenex (Torrance, CA, USA) Jupiter Proteo column (250 × 10 mm, 90 Å) and a linear gradient from 20% to 80% of CH₃CN (0.1% TFA) in H₂O (0.1% TFA) in 30 min at the flow rate of 5 ml/min. Peptide identification and analysis were performed on a Thermo LC-MS LCQ Deca XP MAX instrument (Waltham, MA, USA) equipped with diode array detector combined with an electrospray ion source and a quadrupole mass analyzer using a Phenomenex Jupiter Proteo column (150 × 4.60 mm, 90 Å) and a linear gradient from 20% to 80% of CH₃CN (0.1% TFA) in H₂O (0.1% TFA) in 30 min. The synthesized peptide showed purity above 95%, based on the chromatographic peak area revealed at 210 nm.

MS *m/z* calculated: 1897.0 amu; found 949.4 [M + 2H]²⁺. *R*_t = 18.4 min.

Protein Expression and Purification

VEGFR1_{D2} protein was prepared according to Di Stasi *et al.* [25]. Briefly, VEGFR1_{D2} gene (DNA fragment encoding amino acids 129–229 of the human VEGFR1) was amplified by PCR from cDNA of the full receptor. Then, it was purified and digested with *Nco*I and *Xho*I (New England Biolabs, Ipswich, MA, USA) restriction enzymes. The *Nco*I/*Xho*I gene fragment was ligated into the pETM11 expression vector (EMBL, Hamburg, Germany) downstream to the His-tag and TEV recognition site sequences. The identity of the insert in the resulting recombinant plasmid was confirmed by DNA sequencing (PRIMM, Naples, Italy). The plasmid construct was transformed into *Escherichia coli* BL21 Codon Plus (DE3) RIL cell strain (Stratagene, La Jolla, CA, USA) carrying an inducible T7 RNA polymerase gene. Bacterial culture of 1 l of prewarmed Luria-Bertani medium containing 50 μg ml⁻¹ kanamycin and 33 μg ml⁻¹ chloramphenicol was grown in shaking flasks at 37 °C until reaching 0.7/0.8 OD₆₀₀. Then, they were induced with 0.7-mM IPTG, Isopropyl β-D-1-thiogalactopyranoside

(Inalco, Milan, Italy). After 4–5 h, the cells were harvested by centrifugation; the pellet was dissolved in 50-mM Tris-HCl, pH 8 containing protease inhibitors cocktail (Roche, Basel, Swiss), to avoid protein degradation, and the suspension was sonicated for 6 min, by using a Misonix Sonicator 3000 apparatus (Farmingdale, NY, USA) with a micro tip probe and an impulse output of 1.5/2 (=9/12 W). Bacterial lysate was then centrifuged (27200 g, 30 min, 4 °C), and the inclusion body pellet containing VEGFR1_{D2} was solubilized in 50-mM Tris-HCl, 10-mM imidazole, and 8-mM urea, pH 8. The solubilized VEGFR1_{D2} protein was loaded on a Ni²⁺-NTA resin (45 min, 20 °C) in the presence of 300-mM NaCl. The His-tagged protein was refolded by equilibrating the resin in 50-mM Tris-HCl, 10-mM imidazole, and 300-mM NaCl, pH 8 with decreasing concentrations of urea, and then, it was eluted with increasing imidazole concentration from 100 to 300 mM. The ¹⁵N-labeled recombinant VEGFR1_{D2} was expressed according to Sambrook *et al.* (Sambrook, J.; Fritsch, E. F.; Maniatis, T. *Molecular Cloning*, 2nd ed.; Cold Spring Harbor Laboratory: Cold Spring Harbor, 1989; pp 3, A3). The refolding and protein purification were performed as described for the unlabeled protein. Refolded VEGFR1_{D2} was dialyzed overnight in 50-mM Tris-HCl, pH 7.0 and NaCl 250 mM at 4 °C. Then, the cleavage of the His-tagged protein was performed in the presence of glutathione (3 mM reduced/0.3 mM oxidized) for 3 h at 30 °C, adding a lab prepared Tobacco Etch Virus protease to protein substrate in a molar ratio (protease:substrate) of 1:35. Finally, VEGFR1_{D2} was purified to homogeneity by size exclusion chromatography using a S75 column (GE Healthcare, Milan, Italy) equilibrated in 50-mM Tris-HCl and 250-mM NaCl, pH 7. Finally, it was concentrated until 0.9 mM by the Amicon Ultra system using a membrane with a 3000 MW cut-off (Millipore, Milan, Italy).

NMR Spectroscopy

To map the binding site of MA on VEGFR1_{D2}, ¹⁵N uniformly labeled VEGFR1_{D2} (80 μM in 50-mM Tris-HCl and 250-mM NaCl, pH 7) was titrated with increasing amounts of unlabeled peptide (20, 40, 60, 80, 160, and 240 μM) [26]. Two-dimensional [¹H, ¹⁵N] heteronuclear single quantum coherence (HSQC) spectra were acquired with 32 transients per *t*₁ value. Presaturation of water was employed during a recycle delay of 1.5 s. The 1 K complex points were acquired in *t*₂, with an acquisition time of 102.5 ms, whereas 128 complex points were acquired in *t*₁ with an acquisition time of 64 ms. Backbone ¹⁵N and HN resonance assignments were obtained on the basis of previously reported assignments [27]. To determine the *per* residue chemical shift perturbation upon binding and account for differences in spectral widths between ¹⁵N and ¹H resonances, weighted average chemical shift differences, Δδ_{HN}, were calculated for the amide ¹⁵N and ¹H resonances, using the equation:

$$\Delta\delta_{\text{HN}} = \left[(\Delta\text{HN})^2 + (0.17 \times \Delta^{15}\text{N})^2 \right]^{1/2}$$

where ΔH and ΔN are the differences between the free and bound chemical shifts. The weighted average chemical shift differences were mapped to the VEGFR1_{D2} NMR structure (1QSV.pdb) [27] using MOLMOL graphics program [28]. CARA software [29] was used to generate overlays of the two-dimensional spectra.

The dissociation constants (*K*_d) were estimated from the changes in both ¹H and ¹⁵N chemical shifts as observed in the two-dimensional [¹H, ¹⁵N] HSQC spectra of VEGFR1_{D2} upon binding to MA peptide. The chemical shift changes, measured

at various protein–peptide ratios, were plotted *versus* ligand concentration, and the results were fitted by nonlinear regression according to the following equation [30] with GraphPad Prism, version 4.00 (GraphPad Software, San Diego, CA, USA):

$$\Delta\delta = \Delta\delta_{\max} \left\{ K_d + [P] + [L] - \left[(K_d + [P] + [L])^2 - 4[P][L] \right]^{1/2} / 2[P] \right\}$$

where $\Delta\delta$ is the chemical shift change at various VEGFR1_{D2}/ligand ratios, $\Delta\delta_{\max}$ is the chemical shift change at saturation, K_d is the dissociation constants, and $[P]$ and $[L]$ are the protein and ligand concentrations, respectively. All curve fitting showed an R^2 value ≥ 0.98 .

For NMR STD sample [31], the protein solution was diluted in NMR buffer (50-mM Tris, 100-mM NaCl, and 10% D₂O). The final sample contained 10 μ M of unlabeled VEGFR-1_{D2} and 1-mM peptide, leading to a protein:ligand ratio of 1:100. STD spectra of the unlabeled VEGFR-1_{D2}/peptide complex were recorded with 2048 scans and selective saturation of the protein resonances at 12 and -3 ppm. Time dependence of the saturation transfer was investigated using an optimized saturation times ranging from 0.2 to 4.0 s. STD NMR spectra were acquired using a series of equally spaced 50-ms Gaussian-shaped pulses for selective saturation, with 1-ms delay between the pulses. Subtraction of the protein Free induction decay resonance was performed by phase cycling.

Molecular modeling studies

The HADDOCK web server [32] was used to generate a model of the MA/VEGFR-1_{D2} complex. The NMR structures with the lowest target functions of both MA and VEGFR-1_{D2} (1QSV.pdb) were implemented for these studies. Chemical shift perturbation and STD data were exploited to produce unambiguous interaction restraints. In all of the docking runs, passive residues were set automatically by the HADDOCK web server and the solvated docking mode was turned on. In the first iteration (i.e. the rigid body energy minimization), 1000 structures were calculated; in the second iteration, the best 200 solutions were subjected to semi-flexible simulated annealing, and a final refinement in water was also performed. The final 200 HADDOCK models were all visually inspected, and solutions not compatible with our experimental data and/or containing highly unusual protein orientations were soon removed. In particular, four clusters were obtained, and the best structures of each cluster (according to the HADDOCK score) were compared. Because the resulting structures are very similar to each other, we decided to use the one with the lowest (i.e. best) HADDOCK score as representative of the MA/VEGFR1_{D2} complex.

Results and Discussion

NMR Mapping Studies of the MA Peptide Binding Site on VEGFR1_{D2}

In vitro binding studies showed that MA is able to interact specifically and compete with VEGF for binding site on ECs, therefore indicating that peptide binds to VEGF receptors [21]. To define MA binding site on the receptor and to estimate the complex dissociation constant (K_d), we performed an NMR titration using the second domain of VEGFR1.

Upon progressive additions of unlabeled MA to a sample containing ¹⁵N-labeled VEGFR1_{D2}, we observed continuous changes in ¹H and ¹⁵N chemical shifts for several signals of VEGFR1_{D2} in the two-dimensional ¹H–¹⁵N HSQC spectra (Figure 1). The VEGFR1_{D2} residues showing the most significant changes in ¹H and ¹⁵N chemical shifts upon formation of the complex were assessed by analyzing the normalized chemical shift deviations ($\Delta\delta_{HN}$) and were mapped onto the NMR solution structure of the VEGFR-1_{D2} (Figure 2(A) and (B)). The most affected residues are located in the N-terminal βa strand region encompassing residues from 139 to 145, in the loop separating βc and $\beta c'$ strands (residues 169–172), in the βf strand (residues 204–207), and in the βg strand (residues 216–221). Thus, NMR titration allows us to approximate the region of the VEGFR1_{D2} interacting with the peptide. Notably, this region was involved in the molecular recognition of the VEGF helical region that has been (residues 17–25) exploited to design MA peptide. These chemical shift changes indicated the formation of the MA/VEGFR1_{D2} complex in fast exchange on the NMR time scale. The K_d of the MA/VEGFR1_{D2} complex was estimated to be in the micromolar range ($\approx 46 \pm 13 \mu$ M) after an analysis of the NMR titration curves of selected VEGFR1_{D2} residues (Figure 2(C)).

Binding Epitope of the MA Peptide

To provide information on MA binding residues, one-dimensional STD NMR experiments of MA in the presence of unlabeled VEGFR1_{D2} were performed. As a control experiment, STD NMR spectrum of the peptide without VEGFR1_{D2} protein was recorded. The

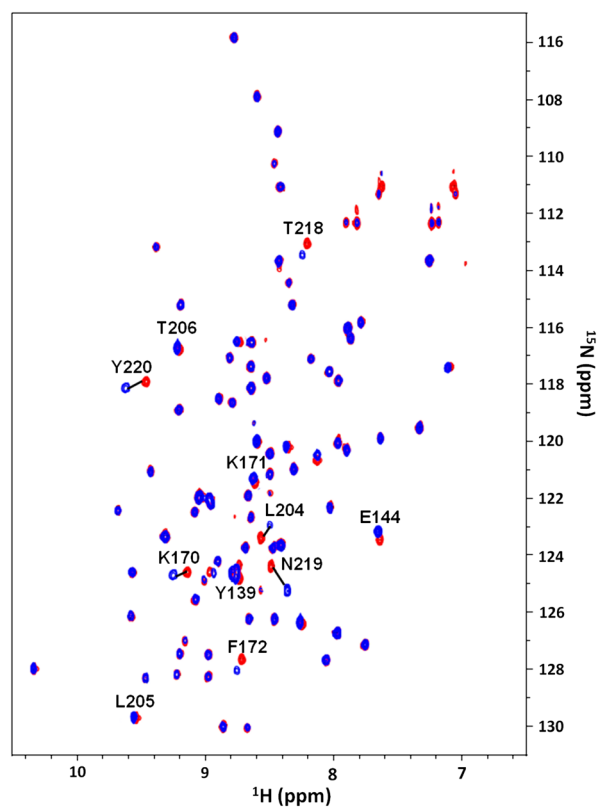


Figure 1. Mapping the VEGFR1_{D2} binding interface for MA. Overlay of [¹H, ¹⁵N] HSQC spectra of ¹⁵N-labeled VEGFR1_{D2} (80 μ M) in absence (red) and presence (blue) of unlabeled peptide MA (80 μ M).

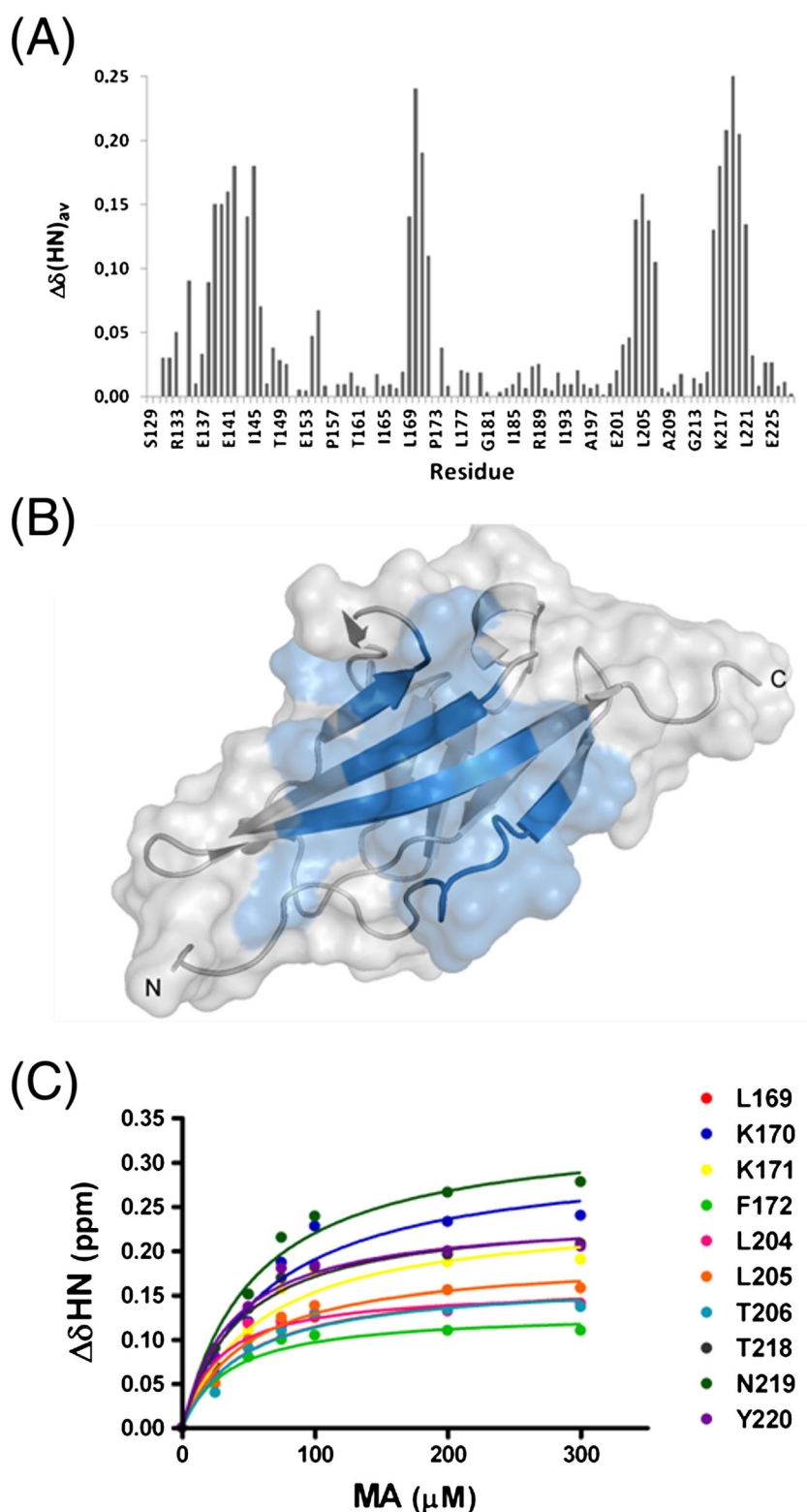


Figure 2. (A) Graph reporting the normalized chemical shift deviations ($\Delta\delta = [(\Delta\text{HN})^2 + (0.17 \times \Delta^{15}\text{N})^2]^{1/2}$) versus the residue. Residues localized at the N-terminal and strand βa (Y139, S140, E141, I142, E144, I145) at the loop between strands βc and $\beta c'$ (L169, K170, K171, and F172), at the strand βf (L204, L205, T206, and C207), and at the strand βg (Y216, K217, T218, N219, Y220, and L221) show normalized deviations with values higher than 0.1 ppm. (B) Amino acids with normalized chemical shifts deviations ($\Delta\delta\text{HN}$ values) greater than 0.1 ppm are colored in blue on the three-dimensional solution structure of VEGFR1_{D2} (conformer number 1, pdb code: 1QSV) in its ribbon and surface representations. (C) Chemical shift changes ($\Delta\delta\text{HN}$) for the H^{15}N resonances of the protein residues showing large variations in chemical shift upon formation of the MA/VEGFR1_{D2} complex as a function of the ligand concentration. The curves represent the best fit solution of the quadratic equation that describes 1:1 complex formation.

sample containing unlabeled VEGFR1_{D2} protein showed saturation transfer from the protein to the ligand in the STD spectra, thus confirming peptide–protein interaction. In particular, the STD spectrum of MA in a 100-fold excess over the unlabeled VEGFR1_{D2} protein (Figure 3) clearly demonstrates the involvement of backbone HN of residues Trp4 and Met5 and of aromatic protons of residues Trp4, Tyr8, and Tyr12. Furthermore, the signal of the H ϵ protons of the side chain of the Gln9 showed similar large STD intensities. All MA residues involved in protein recognition occupy the same face of the helix (Figure 4) and correspond to the interacting residues hypothesized in the design step [24]. The nature of the interacting residues suggests that hydrophobic interactions drive the formation of MA/VEGFR1_{D2} complex.

Molecular Modeling of the MA/VEGFR1_{D2} Complex

To gain structural information about the molecular interface of the bound MA peptide, a structural model of MA/VEGFR1_{D2}

complex has been generated with the HADDOCK web server on the basis of chemical shift perturbation and STD data. Particularly, residues Y139, S140, E141, I142, E144, I145, L169, K170, K171, F172, L204, L205, T206, C207, Y216, K217, T218, N219, Y220, and L221 of the VEGFR1_{D2} and residues W4, Y8, Q9, and Y12 of the MA were considered active. In all of the docking runs, passive residues were set automatically by the HADDOCK web server and the solvated docking mode was turned on. The structure of the complex derived from the molecular modeling studies (Figure 5) shows that the orientation of MA bound to the receptor binding site is consistent with what is observed for the VEGF α 1 helix (residues 17–25) interaction with VEGFR1_{D2} [27]. Moreover, docking results, in agreement with the NMR binding studies, suggest that intermolecular interactions between MA and VEGFR1_{D2} include a network of π – π interactions contacts. Most of these stabilizing hydrophobic intermolecular interactions involve the aromatic ring of the residues Trp4, Tyr8, and Tyr12 of MA peptide and Y139, I145, F172, Y216, L204, Y220, and L221

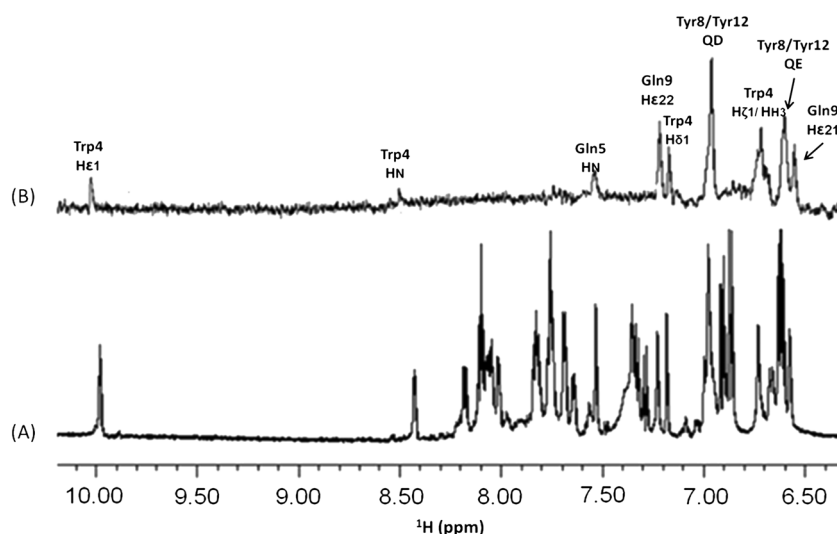


Figure 3. Epitope mapping for MA using one-dimensional STD NMR. Expansions of (A) the reference one-dimensional ¹H NMR spectrum of MA in 50-mM Tris and 100-mM NaCl at pH 7.0 at 298 K and 600 MHz and (B) the NMR STD spectrum of MA in the presence of VEGFR1_{D2} using the same condition as in (A).

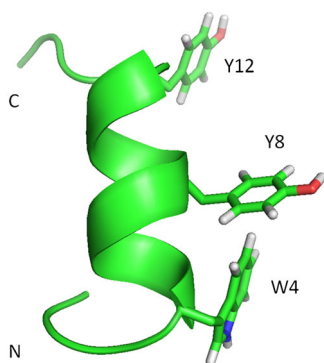


Figure 4. MA binding epitope. The side chain of the residues interacting with the receptor, as revealed by NMR STD experiments, is shown as a neon representation.

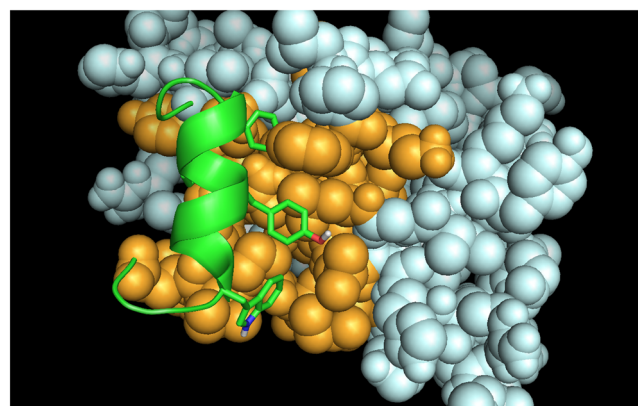


Figure 5. Docking studies. The derived molecular modeling of the MA/VEGFR1_{D2} complex. Residues that are most affected by binding in our chemical shifts perturbation studies ($\Delta\delta_{\text{HN}} > 0.1$ ppm) have been colored in orange on the surface representations of the VEGFR1_{D2}. The side chains of the residues on the MA surface that may contribute to important interactions at the complex interface are shown as a neon representation.

residues on the VEGFR-1_{D2} surface. Potential hydrogen bonds can also be identified involving amide – groups on the VEGFR1_{D2} surface and the hydroxyl group of the tyrosine side chains of the peptide.

Conclusions

The molecular determinants of the binding surface between the helical antagonist peptide MA and VEGFR1_{D2} were examined by combining solution NMR studies and molecular modeling. The peptide binding site on VEGFR1_{D2} has been characterized, and it overlaps with the binding region of VEGF helix 17–25. Furthermore, peptide residues involved in receptor recognition have been determined.

These data demonstrate that to develop peptides targeting protein–protein interactions, an accurate secondary structure motif stabilization keeping the three-dimensional arrangements of the interacting residues may represent a successful structure-based drug design approach. These results provide significant information to develop a new class of molecules able to recognize the VEGF receptors overexpressed in pathological angiogenesis.

Acknowledgements

This work was supported by MIUR (PON Ricerca e Competitività 2007–2013 #PON_01_2388, PRIN 2008-20084MMXNM_004). We thank G. Filograsso, C. Chiarella, L. Zona, and L. De Luca for administrative technical assistance.

References

- 1 Ferrara N, Gerber HP, Le Coutre J. The biology of VEGF and its receptors. *Nat. Med.* 2003; **9**: 669–676.
- 2 Olsson AK, Dimberg A, Kreuger J, Claesson-Welsh L. VEGF receptor signalling – in control of vascular function. *Nat. Rev. Mol. Cell Biol.* 2006; **7**: 359–371.
- 3 Wiesmann C, Fuh G, Christinger HW, Eigenbrot C, Wells JA, de Vos AM. Crystal structure at 1.7 Å resolution of VEGF in complex with domain 2 of the Flt-1 receptor. *Cell* 1997; **91**: 695–704.
- 4 Fuh G, Li B, Crowley C, Cunningham B, James A. Requirements for binding and signaling of the kinase domain receptor for vascular endothelial growth factor. *J. Biol. Chem.* 1998; **273**: 11197–11204.
- 5 Leppänen VM, Prota AE, Jeltsch M, Anisimov A, Kalkkinen N, Strandin T, Lankinen H, Goldman A, Ballmer-Hofer K, Alitalo K. Structural determinants of growth factor binding and specificity by VEGF receptor 2. *Proc. Natl. Acad. Sci. U.S.A.* 2010; **107**: 2425–2430.
- 6 D'Andrea LD, Del Gatto A, Pedone C, Benedetti E. Peptide-based molecules in angiogenesis. *Chem. Biol. Drug Des.* 2006; **67**: 115–126.
- 7 D'Andrea LD, Del Gatto A, De Rosa L, Romanelli A, Pedone C. Peptides targeting angiogenesis related growth factor receptors. *Curr. Pharm. Des.* 2009; **15**: 2414–2429.
- 8 Grothey A, Galanis E. Targeting angiogenesis: progress with anti-VEGF treatment with large molecules. *Nat. Rev. Clin. Oncol.* 2009; **6**: 507–518.
- 9 Folkman J. Angiogenesis. *Annu. Rev. Med.* 2006; **57**: 1–18.
- 10 Folkman J. Angiogenesis: an organizing principle for drug discovery? *Nat. Rev. Drug Discov.* 2007; **6**: 273–286.
- 11 Ferrara N, Kerbel RS. Angiogenesis as a therapeutic target. *Nature* 2005; **438**: 967–974.
- 12 Jacobs J. Combating cardiovascular disease with angiogenic therapy. *Drug Discov. Today* 2007; **12**: 1040–1045.
- 13 Cai W, Chen X. Multimodality molecular imaging of tumor angiogenesis. *J. Nucl. Med.* 2008; **49**: 1135–1285.
- 14 D'Andrea LD, Romanelli A, Di Stasi R, Pedone C. Bioinorganic aspects of angiogenesis. *Dalton Trans.* 2010; **39**: 7625–7636.
- 15 D'Andrea LD, Iaccarino G, Fattorusso R, Sorriento D, Carannante C, Capasso D, Trimarco B, Pedone C. Targeting angiogenesis: structural characterization and biological properties of a *de novo* engineered VEGF mimicking peptide. *Proc. Natl. Acad. Sci. U.S.A.* 2005; **102**: 14215–14220.
- 16 Diana D, Ziaco B, Colombo G, Scarabelli G, Romanelli A, Pedone C, Fattorusso R, D'Andrea LD. Structural determinants of the unusual helix stability of a *de novo* engineered vascular endothelial growth factor (VEGF) mimicking peptide. *Chem. Eur. J.* 2008; **14**: 4164–4166.
- 17 Dudar GK, D'Andrea LD, Di Stasi R, Pedone C, Wallace JL. A vascular endothelial growth factor mimetic accelerates gastric ulcer healing in an iNOS-dependent manner. *Am. J. Physiol. Gastrointest. Liver Physiol.* 2008; **295**: G374–G381.
- 18 Santulli G, Ciccarelli M, Palumbo G, Campanile A, Galasso G, Ziaco B, Altobelli GG, Cimini V, Piscione F, D'Andrea LD, Pedone C, Trimarco B, Iaccarino G. In vivo properties of the proangiogenic peptide QK. *J. Transl. Med.* 2009; **7**: 41–50.
- 19 Diana D, Ziaco B, Scarabelli G, Pedone C, Colombo G, D'Andrea LD, Fattorusso R. Structural analysis of a helical peptide unfolding pathway. *Chem. Eur. J.* 2010; **16**: 5400–5407.
- 20 Gautier B, Goncalves V, Diana D, Di Stasi R, Teillet F, Lenoir C, Huguenot F, Garbay C, Fattorusso R, D'Andrea LD, Vidal M, Inguibert N. Biochemical and structural analysis of the binding determinants of a vascular endothelial growth factor receptor peptidic antagonist. *J. Med. Chem.* 2012; **53**: 4428–4440.
- 21 Basile A, Del Gatto A, Diana D, Di Stasi R, Falco A, Festa M, Rosati A, Barbieri A, Franco R, Arra C, Pedone C, Fattorusso R, Turco MC, D'Andrea LD. Characterization of a designed vascular endothelial growth factor receptor antagonist helical peptide with antiangiogenic activity in vivo. *J. Med. Chem.* 2011; **54**: 1391–1400.
- 22 Ziaco B, Diana D, Capasso D, Palumbo R, Celentano V, Di Stasi R, Fattorusso R, D'Andrea LD. C-terminal truncation of vascular endothelial growth factor mimetic helical peptide preserves structural and receptor binding properties. *Biochem. Biophys. Res. Commun.* 2012; **424**: 290–294.
- 23 Finetti F, Basile A, Capasso D, Di Gaetano S, Di Stasi R, Pascale M, Turco CM, Ziche M, Morbidelli L, D'Andrea LD. Functional and pharmacological characterization of a VEGF mimetic peptide on reparative angiogenesis. *Biochem. Pharmacol.* 2012; **84**: 303–311.
- 24 Diana D, Basile A, De Rosa L, Di Stasi R, Auriemma S, Arra C, Pedone C, Turco MC, Fattorusso R, D'Andrea LD. β-hairpin peptide that targets vascular endothelial growth factor (VEGF) receptors: design, NMR characterization, and biological activity. *J. Biol. Chem.* 2011; **286**: 41680–41691.
- 25 Di Stasi R, Diana D, Capasso D, Palumbo R, Romanelli A, Pedone C, Fattorusso R, D'Andrea LD. VEGFR1(D2) In drug discovery: expression and molecular characterization. *Biopolymers* 2010; **94**: 800–809
- 26 Pellecchia M, Bertini I, Cowburn D, Dalvit C, Giralt E, Jahnke W, James TL, Homans SW, Kessler H, Luchinat C, Meyer B, Oschkinat H, Peng J, Schwalbe H, Siegal G. Perspectives on NMR in drug discovery: a technique comes of age. *Nat. Rev. Drug Discov.* 2008; **7**: 738–745.
- 27 Starovasnik MA, Christinger HW, Wiesmann C, Champe MA, De Vos AM, Skelton NJ. Solution structure of the VEGF-binding domain of Flt-1: comparison of its free and bound states. *J. Mol. Biol.* 1999; **293**: 531–544.
- 28 Koradi R, Billeter M, Wüthrich K. MOLMOL: a program for display and analysis of macromolecular structures. *J. Mol. Graph.* 1996; **14**: 29–32.
- 29 Masse JE, Keller R. AutoLink: automated sequential resonance assignment of biopolymers from NMR data by relative-hypothesis-prioritization-based simulated logic. *J. Magn. Reson.* 2005; **174**: 133–151.
- 30 Morton CJ, Pugh DJ, Brown EL, Kahmann JD, Renzoni DAC, Campbell ID. Solution structure and peptide binding of the SH3 domain from human Fyn. *Structure* 1996; **4**: 705–714.
- 31 Klages J, Coles M, Kessler H. NMR based screening: a powerful tool in fragment-based drug discovery. *Mol. Biosyst.* 2006; **2**: 318–23.
- 32 Dominguez C, Boelens R, Bonvin AM. HADDOCK: a protein-protein docking approach based on biochemical or biophysical information. *J. Am. Chem. Soc.* 2003; **125**: 1731–1737.